SpezialForschungsBereich F 32

Karl–Franzens Universität Graz
Technische Universität Graz
Medizinische Universität Graz

On Theoretical Limits in Parallel Magnetic Resonance Imaging

Frank Bauer Christian Clason

SFB-Report No. 2008–024 December 2008

A–8010 GRAZ, HEINRICHSTRASSE 36, AUSTRIA

Supported by the
Austrian Science Fund (FWF)

Der Wissenschaftsfonds.

SFB sponsors:

- **Austrian Science Fund** (FWF)
- **University of Graz**
- **Graz University of Technology**
- **Medical University of Graz**
- **Government of Styria**
- **City of Graz**

On Theoretical Limits in Parallel Magnetic Resonance Imaging

Frank Bauer and Christian Clason

***Abstract*—Based on a Fourier series expression of true image, receiver sensitivities, and measurements, it is possible to give theoretical limits for the perfect reconstructability of image and sensitivities in parallel magnetic resonance imaging. These limits depend on the smoothness of the sensitivities, number of receiver coils, and size of the acquired k-space measurement window. Different types of a priori information can be incorporated in the determination of these limits. Furthermore, the method employed is constructive and can serve as the basis for a nonlinear reconstruction scheme, as is shown using data from a simulated phantom.**

***Index Terms*—Magnetic resonance imaging, Image reconstruction, Fourier series, Newton method**

I. Introduction

MAGNETIC Resonance Imaging (MRI) is a medical imaging method which employs radio pulse echoes to measure the hydrogen atom density, which allows the discrimination of different types of tissue. The spatial information is encoded, using a combination of gradient magnetic fields, in the phase and frequency of the time-dependent echo, which is then measured by coils surrounding the patient. A Fourier transform of the recorded signal will therefore yield – line by line – an image of the investigated area (for a full discussion of the principles of MRI, see, e.g., [1], [2]). One of the major drawbacks of MRI in current practice is the speed of the image acquisition, since each line has to be acquired separately. The standard approach for speeding up the process acquires a subset of the lines (e.g., every second or every fourth). This, however, leads to aliasing, as the two-dimensional signal is now sampled below the Nyquist frequency (cf. Fig. 1 and the above references). As a remedy, Parallel Magnetic Resonance Imaging (PMRI) measures the radio echo using multiple complementary coils, which are usually placed in a circle around the patient. Since these coils have only limited aperture compared to a single coil, the resulting measurements are non-uniformly modulated. In this way one hopes to make up for the lost information.

Reconstruction strategies currently in use in daily clinical practice include SENSE [3], which is an algebraic linear least-squares recovery of the unaliased image using sensitivities taken from a fully sampled reference scan, and GRAPPA [4], where the missing Fourier coefficients are interpolated using an interpolation kernel fitted to additionally acquired lines around the zero frequency (in effect this is also fully sampled low-resolution reference scan). The quality of reconstruction therefore depends on the number of these so-called center lines, which reduces the speed-up gained from subsampling. Recently, nonlinear least squares methods for PMRI have been proposed [5], [6], [7], which treat the sensitivities as additional unknowns and were shown to allow improved reconstructions. Common to all algebraic reconstruction techniques is the danger of ghost respectively overfolding artifacts, which arise from incomplete separation of the superimposed parts in the aliased image (illustrated in Fig. 1d for a naive Tikhonov-regularized least squares solution using known sensitivities). In practice, of course, achievable reconstruction is also limited by physical constraints such as the signal-to-noise ratio (SNR), see, e.g., [8]. In the case of well known sensitivities there exists an extensive literature (e.g. [9], [10], [11]) giving account on the SNR of the reconstructions. In particular the noise imposed by measurement noise just depends mildly [9] on the undersampling.

In contrast to these works, we consider, as in GRAPPA and [7], the sensitivities as unknown and focus on the error imposed by the overfolding artifacts. We start by considering theoretical limits for the acceleration factor, in the sense that we derive algebraically necessary conditions under which it is in principle still possible, with a given number of receiver coils, to reconstruct image and sensitivities perfectly. It will be shown that this limit also depends in non-trivial ways on the smoothness of the sensitivities and the desired resolution. The main contribution of this work is thus to give guidelines for choosing appropriate set-ups for parallel imaging, which might be helpful both for SENSE and GRAPPA like methods. Additionally, the presented constructive approach can serve as the basis for the development of new reconstruction methods.

II. Theory

A. Mathematical model and problem formulation

We consider the true image P as a function in $L^2([-1,1]^2)$. Since usually subsampling is only performed in one direction, we will treat the image as being composed of independent lines parallel to the aliasing direction,

F. Bauer is with the Fuzzy Logic Laboratorium, Johannes Kepler University of Linz, Softwarepark 21, 4232 Hagenberg, Austria (phone: ++43 7236 3343 432; fax: ++43 7236 3343 434; email: frank.bauer@jku.at). His work was supported by the Upper Austrian Technology and Research Promotion

C. Clason is with the Institute for Mathematics and Scientific Computing, University of Graz, Heinrichstrasse 36, A-8010 Graz, Austria, (email: christian.clason@uni-graz.at). His work was supported by the Austrian Science Fund (FWF) under grant SFB F32.

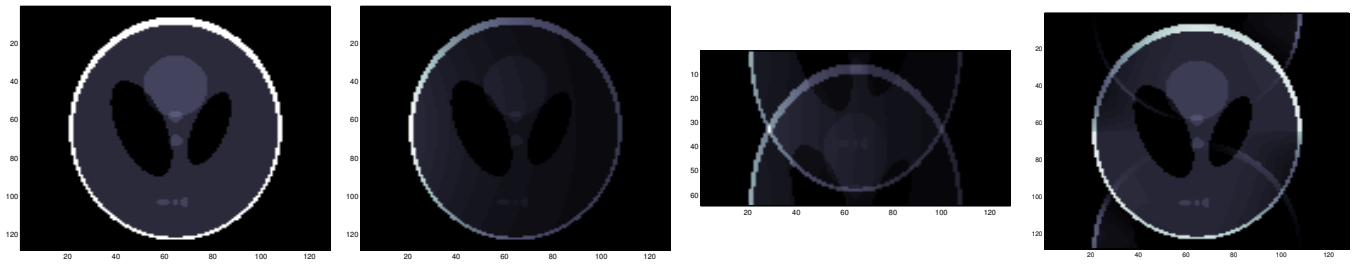

(a) (b) (c) (d)

Fig. 1. Illustration of modulation and aliasing applied to a phantom: (a) True image, (b) modulated coil image, (c) modulated and sub-sampled (factor 2) coil image, (d) naive reconstruction suffering from ghost artifacts.

which can be expressed as a Fourier series

$$P(x) = \sum_{k=-\infty}^{\infty} p_k e^{ikx},$$

where we assume that at most N_P+1 coefficients are non-zero. This allows us to write

$$P(x) = \sum_{k=-\lfloor N_P/2 \rfloor}^{\lceil N_P/2 \rceil} p_k e^{ikx},$$

where w.l.o.g. for odd N_P, we distribute the additional asymmetric coefficient to the positive part of the sum.

Similarly, let C be the number of receiver coils, with corresponding coil sensitivities $R^j \in L^2([-1,1]^2)$, $j = 1,\dots,C$, each of which can be written as

$$R^j(x) = \sum_{k=-\lceil N_R/2 \rceil}^{\lfloor N_R/2 \rfloor} r_k^j e^{ikx}, \qquad j = 1,\dots,C.$$

Again, N_R+1 is the maximal number of non-zero coefficients for all sensitivities. We make the additional assumption that the sensitivities are much smoother than the image, i.e., that $N_R \ll N_P$, which in practice is always the case. Here, the excess coefficient for odd N_R is counted for the negative part of the sum.

A full measurement now consists of the Fourier coefficients of the point-wise multiplication of P and R_j. This is expressed as:

$$\begin{aligned}\sum_{k=-\lfloor N_P/2 \rfloor-\lceil N_R/2 \rceil}^{\lceil N_P/2 \rceil+\lfloor N_R/2 \rfloor} m_k^j e^{ikx} = M^j(x) = R^j(x)\cdot P(x)\\ = \sum_{k=-\lfloor N_P/2 \rfloor}^{\lceil N_P/2 \rceil} \sum_{l=-\lceil N_R/2 \rceil}^{\lfloor N_R/2 \rfloor} p_l r_k^j e^{i(l+k)x}\end{aligned}$$

Simple manipulation then yields

$$m_k^j = \sum_{\substack{a+b=k \\ -\lfloor N_P/2 \rfloor \le a \le \lceil N_P/2 \rceil \\ -\lceil N_R/2 \rceil \le b \le \lfloor N_R/2 \rfloor}} p_a r_b^j \qquad (1)$$

In parallel MRI, only a subset of these coefficients are measured, which we denote by the index set $U \subset \{-\lfloor N_P/2 \rfloor - \lceil N_R/2 \rceil, \dots, \lceil N_P/2 \rceil + \lfloor N_R/2 \rfloor\}$ which yields for $j = 1\dots,C$

$$\begin{aligned}\mathcal{S}_U\left(R^j(x)\cdot P(x)\right) = M_U^j(x)\\ = \sum_{k=-\lfloor N_P/2 \rfloor-\lceil N_R/2 \rceil}^{\lceil N_P/2 \rceil+\lfloor N_R/2 \rfloor} \delta_{k\in U}\, m_k^j e^{ikx}.\end{aligned}$$

In standard applications we normally have an equidistant subsampling, i.e.

$$U = \left\{ -\lfloor \frac{N_P}{2} \rfloor - \lceil \frac{N_R}{2} \rceil \le k \le \lceil \frac{N_P}{2} \rceil + \lfloor \frac{N_P}{2} \rfloor \,\middle|\, k/S \in \mathbb{Z} \right\},$$

where S is the so-called acceleration factor. In all other cases we define $S := (N_P + N_R + 1)/|U|$.

Actually, an MR scanner physically determines exactly these coefficients m_k^j; the sampling strategy (i.e., the decision which lines to measure) directly corresponds to a specific choice of U.

Since we are interested in theoretical limitations, we assume in the following that, regardless of subsampling, all $N_R + N_P + 1$ coefficients are acquired. Lower numbers (e.g., $N_P + 1$) can easily be treated by a modification of the index set U.

The problem we consider is now the following:

Problem 2.1: Given N_P, N_R and C, find the largest number S such that knowledge of

$$m_k^j\,, \qquad k \in U, \quad j = 1\dots,C$$

can still determine uniquely

$$p_k\,, \qquad k = -\lfloor N_P/2 \rfloor, \dots, \lceil N_P/2 \rceil$$

and for $j = 1\dots,C$

$$r_k^j\,, \qquad k = -\lceil N_R/2 \rceil, \dots, \lfloor N_R/2 \rfloor.$$

B. Minimum requirements for PMRI

Now we make use of the representation (1) to derive bounds on the acceleration factor S for which the resulting system of algebraic equations is uniquely solvable for p_k and r_k^j. To be precise, we derive necessary conditions which hold in the absence of any a priori information (like positivity or upper physical bounds) which might implicitly be used in specific algorithms.

1) Number of unknowns: A number of important MRI applications rely on image phase to provide critical information. A partial list includes proton resonance-based MR temperature mapping, phase-contrast velocity mapping for flow imaging in MR angiography, Dixon water/fat imaging, and phase-sensitive inversion recovery MRI (cf. [12]). Hence, in general, we have to assume that not only the coil sensitivities (and hence the measurements) but also the image is complex.

Thus, we need to reconstruct all N_c unknown coefficients,

$$N_c = N_P + CN_R + C + 1.$$

2) Available equations: By the given Fourier coefficients of the measurement, we have in total

$$N_E := C \cdot |U| = C\frac{N_P + N_R + 1}{S}$$

algebraic equations.

3) Algebraic conditions: According to the discussion above, we have in total N_E equations to determine N_c unknown coefficients. On the one hand, a system of n polynomials of degree m in n complex variables will have (with probability 1) exactly m^n different solutions [13]. On the other hand, a system of $n+1$ polynomials in n variables will in general have no solution. However, since we know that (in the absence of noise) the right hand side is by construction equal to the left hand side for the true image and sensitivities, we are in this special case always guaranteed the existence of at least one solution.

Therefore, a necessary condition for the unique solvability of this system of equations, and hence the reconstructability of P and R^j, is that the number of equations is strictly greater than the number of unknowns:

$$N_E > N_c.$$

This, of course, assumes that the receivers are linearly independent in the mathematical sense (for this, it is sufficient for the coil sensitivities to have complementary spatial variation, even if the receivers are not completely independent due to electromagnetic coupling and common noise). Due to the bilinear structure of the problem, adding a linearly dependent receiver does not contribute any additional information and hence will not increase N_E. In particular, this means that for the purpose of increasing the possible acceleration factor, at most $N_R + 1$ receivers can be used. (Naturally, more coils can be useful in other respects like noise reduction).

III. Results

If C, N_P, N_R are given, that means the highest possible acceleration factor S must satisfy

$$S < \frac{CN_P + CN_R + C}{N_P + CN_R + C + 1}$$

This allows us immediately to make the following observations:

1) Given arbitrarily fine resolution, i.e., $N_P \to \infty$, the maximal acceleration factor is equal to the number of coils, as expected. However, in any finite setting the maximal acceleration factor is *always* strictly smaller than the number of coils.
2) If N_P and C is fixed, S is determined by the smoothness of R^j. Specifically, the lower N_R, the larger the acceleration factor can be chosen. For twelve coils, $N_P = 256$ and $N_R = 16$ will theoretically allow $S = 7$, while the same N_P and $N_R = 128$ limits the acceleration factor to $S = 2$.
   In general, if $N_R = \alpha N_P$ for some $0 < \alpha \leq 1$, we have
   $$S_C(\alpha) = \frac{N_P C(1+\alpha) + C}{C\alpha N_P + N_P + C + 1} \tag{2}$$
   Fig. 2a shows this function for different values of C and $N_P = 256$.
   This behavior is understandable, since given the product $M = P \cdot R$, any factor of M having only N_R non-zero Fourier coefficients could be part of either P or R, and a unique recovery is not possible without additional constraints (such as adding additional independent measurements) or a priori information (such as an approximate measurement of the sensitivities).
   Another interesting observation is, that adding more receivers does not give as much information as desired when the receivers are not very smooth (i.e. N_R is very small).

If, on the other hand, a specific acceleration factor S is desired, we can give a lower bound on the number of receiver coils necessary:

$$C > \frac{SN_P + S}{N_P + N_R + 1 - SN_R - S}.$$

Commonly, only $N_P + 1$ frequencies are acquired. In this case, we have the following limits:

$$S < \frac{CN_P + C}{N_P + CN_R + C + 1}$$

For arbitrarily fine image resolution, the maximal acceleration factor is still equal to the number of coils. For finite N_P, however, the achievable acceleration factor will be lower

$$S_C(\alpha) = \frac{N_P C + C}{C\alpha N_P + N_P + C + 1}$$

(in the example above, $S = 6$ and $S = 1$, respectively). Fig. 2b gives the maximal S in for various coil numbers and $N_P = 256$ for this situation. We see that we lose at most one acceleration factor compared to maximal acquisition.

The minimal number of receiver coils for a desired acceleration factor can be estimated by

$$C > \frac{SN_P + S}{N_P + 1 - SN_R - S}.$$

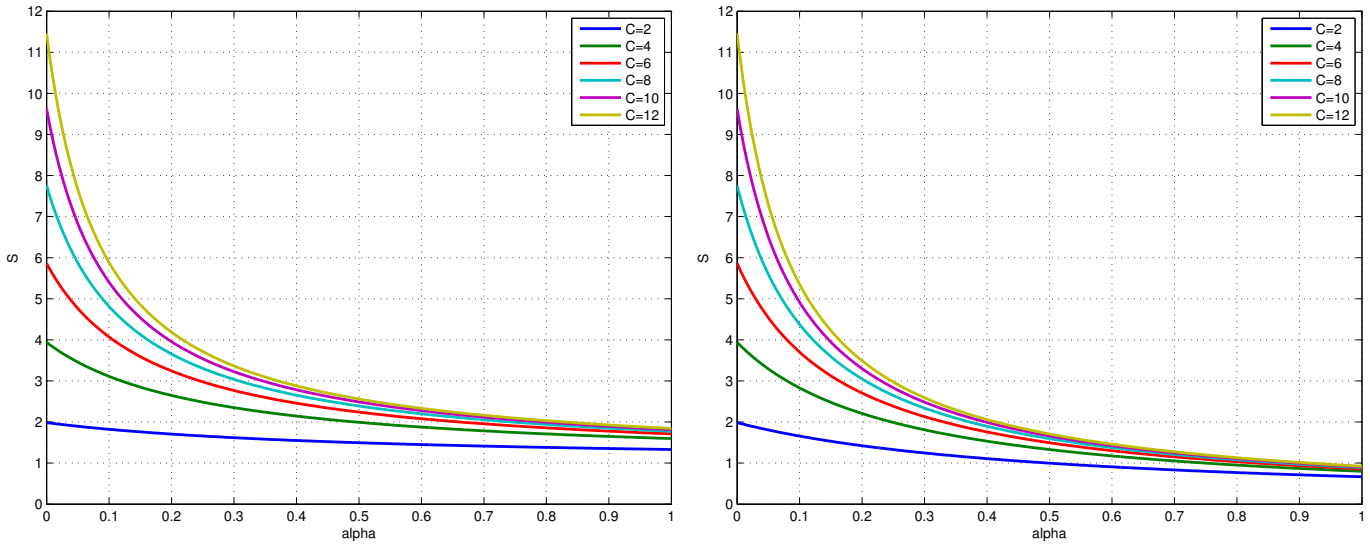

(a) (b)

Fig. 2. Maximal acceleration factor S depending on sensitivity smoothness $N_R = \alpha N_P$ for different coil numbers C and $N_P = 256$: (a) $N_P + N_R + 1$ lines are acquired, (b) $N_P + 1$ lines are acquired.

A. Incorporating a priori information

If one has further a priori information on the image or the sensitivities, it is possible to use this information to improve reconstructability. In our model, such information can be considered as additional equations.

1) Scaling invariance: The image and the sensitivities are only unique up to a constant factor, and one is in general only interested in relative, not absolute contrast in the image. Usually, this is treated by renormalization of the recovered image. Hence we can fix this factor by setting, e.g. $p_0 = 1$, which yields one additional equation.

This consideration also indicates that the bounds derived above are really just necessary conditions, as we cannot rule out that there are much more complicated hypersurfaces in the space of possible coefficients which all yield the same measurement and hence are not distinguishable.

2) Real images: If we can assume the image to be real (as, e.g., in standard MRI situations), we have additional information which gives us in total another $\lfloor N_P/2 \rfloor$ equations

$$p_{-k} = \overline{p_k}$$

for $0 \leq k \leq \lfloor N_P/2 \rfloor$ (in particular, p_0 is real).

Now we have

$$N_E = \frac{C(N_P + N_R + 1)}{S} + \lfloor N_P/2 \rfloor$$

conditions, which lead to the bound

$$S < \frac{C(N_P + N_R + 1)}{\lceil N_P/2 \rceil + CN_R + C}.$$

1) Surprisingly, for $N_P \to \infty$, we have now that S can be equal to $2C$.
2) The maximum achievable acceleration factor for finite resolutions is higher as well, but profits the less the coarser the sensitivities are: e.g., $S = 9$ for $N_P = 256$ and $N_R = 16$, but still only $S = 2$ for $N_P = 256$ and $N_R = 128$. In general:

$$S_C(\alpha) = \frac{CN_P(1+\alpha) + C}{N_P(1/2 + C\alpha) + C},$$

the behavior of which is shown in Fig. 3a.

Again, acquiring only $N_P + 1$ instead of $N_P + N_R + 1$ k-space coefficients will at most decrease the maximum achievable acceleration factor by one.

3) Receiver normalization: In many MR scanners one tries to guarantee pointwise approximately the following identity:

$$\sum_{j=1}^{C} R^j = 1$$

which yields an additional set of $N_R + 1$ equations

$$\sum_{j=1}^{C} r_k^j = \delta_{0k}.$$

When one just tries to guarantee pointwise

$$\sum_{j=1}^{C} |R^j|^2 = 1$$

the underlying equations get a bit more complicated, however, this yields effectively just a set of another $N_R/2$ equations.

B. A numerical reconstruction scheme

The representation (1) can also be used as the basis for a numerical reconstruction scheme for parallel MR imaging, by considering (1) as a nonlinear system of equations

$$f(\mathcal{P}, \mathcal{R}) = \mathcal{M}$$

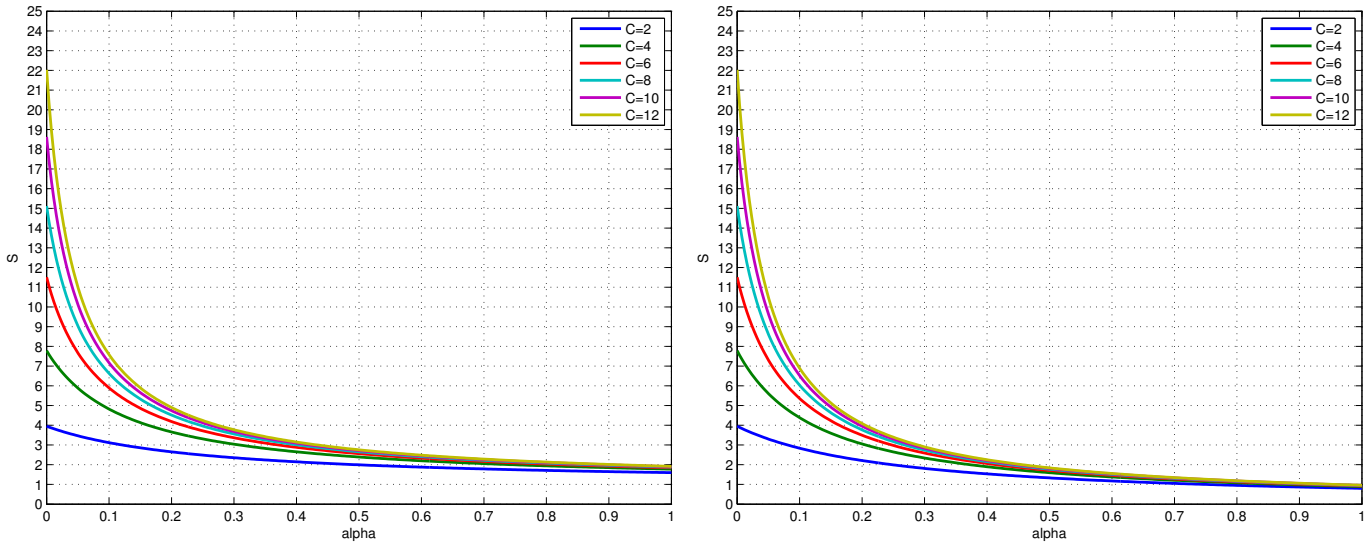

(a) (b)

Fig. 3. Maximal acceleration factor S depending on sensitivity smoothness $N_R = \alpha N_P$ for real images: (a) $N_P + N_R + 1$ lines are acquired, (b) $N_P + 1$ lines are acquired.

for the unknown $\mathcal{P} = (p_l)_l$ and $\mathcal{R} = (r_k^j)_{j,k}$ and given $\mathcal{M} = (m_k^j)_{j,k\in U}$. In matrix notation, this can be written as

$$f(\mathcal{P},\mathcal{R}) = ((f(\mathcal{P},\mathcal{R}))_1,\dots,(f(\mathcal{P},\mathcal{R}))_C)^T,$$

$$(f(\mathcal{P},\mathcal{R}))_j = \mathcal{S}_{\mathcal{U}} \begin{pmatrix} r^j_{-\lceil \frac{N_R}{2}\rceil} & & & \\ r^j_{-\lceil \frac{N_R}{2}\rceil+1} & r^j_{-\lceil \frac{N_R}{2}\rceil} & & \\ \vdots & \vdots & \ddots & \vdots \\ & & & r^j_{\lfloor \frac{N_R}{2}\rfloor} \end{pmatrix} \begin{pmatrix} p_{-\lfloor \frac{N_P}{2}\rfloor} \\ \vdots \\ p_{\lceil \frac{N_P}{2}\rceil} \end{pmatrix} \quad (3)$$

or equivalently as

$$(f(\mathcal{P},\mathcal{R}))_j = \mathcal{S}_{\mathcal{U}} \begin{pmatrix} p_{-\lfloor \frac{N_P}{2}\rfloor} & & & \\ p_{-\lfloor \frac{N_P}{2}\rfloor+1} & p_{-\lfloor \frac{N_P}{2}\rfloor} & & \\ \vdots & \vdots & \ddots & \vdots \\ & & & p_{\lceil \frac{N_P}{2}\rceil} \end{pmatrix} \begin{pmatrix} r^j_{-\lceil \frac{N_R}{2}\rceil} \\ \vdots \\ r^j_{\lfloor \frac{N_R}{2}\rfloor} \end{pmatrix}.$$

where $\mathcal{S}_{\mathcal{U}}$ is the subsampling operator as described beforehand (which removes rows corresponding to not measured coefficients).

Since we have more equations than unknowns, we want to solve this by an iteratively regularized Gauß-Newton method [14], [6], [7], i.e., by computing

$$\min_{(\delta\mathcal{P},\delta\mathcal{R})} \frac{1}{2}\|f'(\mathcal{P}_n,\mathcal{R}_n)(\delta\mathcal{P},\delta\mathcal{R})^T - \mathcal{M} + f(\mathcal{P}_n,\mathcal{R}_n)\|^2 + \frac{\alpha_k}{2}\|(\mathcal{P}_n,\mathcal{R}_n) + (\delta\mathcal{P},\delta\mathcal{R}) - (\mathcal{P}_0,\mathcal{R}_0)\|^2$$

and setting $(\mathcal{P}_{n+1},\mathcal{R}_{n+1}) := (\mathcal{P}_n,\mathcal{R}_n)+(\delta\mathcal{P},\delta\mathcal{R})$, $\alpha_{k+1} := q\alpha_k$ with $0 < q < 1$. The corresponding iteration can be reformulated as

$$\begin{aligned}(\mathcal{P}_{n+1},\mathcal{R}_{n+1}) = (\mathcal{P}_0,\mathcal{R}_0) &+ (f'(\mathcal{P}_n,\mathcal{R}_n)^* f'(\mathcal{P}_n,\mathcal{R}_n) + \alpha_n)^{-1} \\ &f'(\mathcal{P}_n,\mathcal{R}_n)^*\big[\mathcal{M} - f(\mathcal{P}_n,\mathcal{R}_n) \\ &+ f'(\mathcal{P}_n,\mathcal{R}_n)((\mathcal{P}_n,\mathcal{R}_n) - (\mathcal{P}_0,\mathcal{R}_0))\big],\end{aligned}$$

which in practice is slightly faster to evaluate as well as more stable.

The derivative $f'(\mathcal{P},\mathcal{R})$ acting on an increment $(\delta\mathcal{P},\delta\mathcal{R})^T = (\mathcal{P}_{n+1}-\mathcal{P}_n, \mathcal{R}_{n+1}-\mathcal{R}_n)^T$ can be calculated explicitly using the product rule:

$$(f'(\mathcal{P},\mathcal{R})(\delta\mathcal{P},\delta\mathcal{R}))_{k,j} = \sum_{a+b=k} \delta p_a r_b^j + \sum_{a+b=k} p_a \delta r_b^j,$$

or in brief

$$f'(\mathcal{P},\mathcal{R})(\delta\mathcal{P},\delta\mathcal{R}) = f(\mathcal{P},\delta\mathcal{R}) + f(\delta\mathcal{P},\mathcal{R}).$$

Hence, the derivative can be applied very quickly. Similarly, the evaluation of the adjoint derivative is rather straight forward and fast:

$$f'(\mathcal{P},\mathcal{R})^*(\delta\mathcal{M}) = \Big(\sum_{i=1}^{C} f^*(\mathcal{S}_{\mathcal{U}}^*\delta\mathcal{M}_i, R), f^*(P,\mathcal{S}_{\mathcal{U}}^*\delta\mathcal{M}_1),\dots,f^*(\mathcal{P},\mathcal{S}_{\mathcal{U}}^*\delta\mathcal{M}_C)\Big)^T,$$

where f^* is the multiplication with the Hermitian matrix corresponding to the appropriate matrix in (3) and $\mathcal{S}_{\mathcal{U}}^*$ is the operator inserting zeros at non-measured parts.

Note that this method parallelizes trivially, since all lines along the fully sampled directions can be treated independently. Additionally, since only single lines are considered, the problem size is reduced significantly compared to a full image reconstruction: For standard image

sizes, the iteration matrices fit inside the cache memory. In fact, due to the enormous parallelism inherent in this approach (hundreds of independent lines for a single slice, thousands for a full 3D data set) and the data locality, this method is well suited for implementation on graphics hardware. Another advantage of this approach over an image space based method is that the receiver sensitivities are determined by the measurements even in points x for which $P(x) = 0$ holds, due to the nonlocal coupling via the Fourier coefficients. On the other hand, it is possible to introduce coupling between neighboring lines as a penalty, which could be expected to give more stability in the presence of noise. Since this reduces the parallelizability, the trade-off should be considered in specific cases.

C. Numerical experiments

We show the feasibility of this approach by applying the proposed method for a single aliased line of the standard Shepp-Logan phantom (cf. Fig. 1). Setting $N_P = 256$ and $N_R = 10$ and measuring all $N_P + N_R + 1$ coefficients, the discussion in section II-B shows that using $C = 2, 3, 4, 5$ coils, the limiting acceleration factors are $S = 1.9140, 2.7621, 3.5482, 4.2788$ respectively—smaller factors should allow reconstruction, while larger factors should lead to failure.

We illustrate this using the one-dimensional Fourier transform of a single line from the Shepp-Logan phantom and random sensitivities (real and imaginary part normally distributed with mean zero and variance one). We start at a randomly perturbed image and sensitivity, and calculate new iterates using the IRGNM until the norm of the residual drops below 10^{-4}. The iteration converged in every case. We then plot the inverse Fourier transform of $\mathcal{P}$. Since the reconstruction can be unique only up to a constant, we rescale the transform such that the maximal value is one. The results are shown in Fig. 4, where the blue line shows the good reconstruction achievable with an acceleration factor chosen according to the calculations above, while the red line shows failed reconstructions for acceleration factors chosen too large.

To close this section, we show the reconstruction of a full 2D image using the described method. We generated the measurements sequentially from the (vertical) lines of a Shepp-Logan phantom with a resolution of $N_P = 128$. The receiver sensitivities (with $N_R = 6$) were independently and randomly generated for each of these lines and $C = 12$ coils, and the resulting measurements subsampled with an acceleration factor of $S = 4$. As is usual in parallel MRI, we had to include center lines to achieve complete removal of aliasing artifacts if starting too far from the true solution (cf. Fig. 5a, which clearly shows aliasing artifacts). Here the central 3 coefficients sufficed. The result, reconstructed line by line, is shown in Fig. 5b, which is visually indistinguishable from the true image. To show the feasibility of parallelization, we started the computation of each line from the same constant initial guess $p_i = 0$, $r_i = 1$. Taking the previous line as the initial guess naturally leads to faster convergence for each line. While this of course is still far from an actual reconstruction of parallel imaging data, it shows the promise of our approach for the development of a novel reconstruction method.

IV. Discussion

In practical situations we face two major problems. On the one hand, the measurements are perturbed by noise, and on the other hand, although the sensitivities are very smooth, they still can have a rather large (most likely infinite) number of non-zero Fourier coefficients. Another problem which will occur in practice is that we actually do not know the number of relevant Fourier coefficients of the Receivers N_R exactly. This can lead to another kind of non-uniqueness: There might be two reconstructions with different receiver sizes which lead to exactly the same measurements, but which are completely different when looking at the image respectively the receiver coefficients.

However, a quick calculation using δ_k^j as the noise on the exact measurement m_k^j shows:

$$\overline{m_k^j} = \sum_{a+b=k} p_a r_b^j + \delta_k^j$$

and thus

$$|\overline{m_k^j} - m_k^j| \leq |\delta_k^j| + \|\mathcal{P}\|\|\mathcal{R}_j|_{N_R}\| + \|\mathcal{P}|_{N_P}\|\|\mathcal{R}_j\| + \|\mathcal{P}|_{N_P}\|\|\mathcal{R}_j|_{N_R}\|$$

where $\mathcal{R}_j|_{N_R}$ denotes the high-pass filtered version of $\mathcal{R}_j$ without the first N_R Fourier coefficients, and similarly $\mathcal{P}|_{N_P}$ are the coefficients of the high-pass filtered image.

This means that as long as the amplitude of the higher Fourier coefficients is lower than the noise level, we can ignore these without further loss. Interestingly, this also means that noise limits the theoretical possibilities of undersampling perhaps in a severe way (cf. also [8]).

In practice, the dual issue of non-uniqueness and missing knowledge of the number of relevant Fourier coefficients could be dealt with by adding a sparsity constraint [15], which was not necessary in our test problems.

1) Center Lines: Indeed, the assumption that high frequency coefficients have lower amplitude than the central frequencies can be observed in virtually all realistic images and receiver sensitivities. In this case, the implicit assumption that all measured coefficients are of equal value, and that the sampling strategy can be completely specified by the number of measured coefficients, is no longer valid. Instead, it is then vital to acquire center lines, as can be explained using equation (1): If both the image and the sensitivity have very small Fourier coefficients outside the central (let's say 3) frequencies, only the terms $p_1 r_1$, $p_1 r_0$, $p_0 r_1$, $p_0 r_0$, and the corresponding terms involving the index -1 instead of 1 will be non-negligible. That implies that this information is only contained in the coefficients m_{-2}, m_{-1}, m_0, m_1 and m_2, although the coupling theoretically extends to more terms. So the omission of any of them due to the subsampling will lead to loss of uniqueness, even though the number of coils

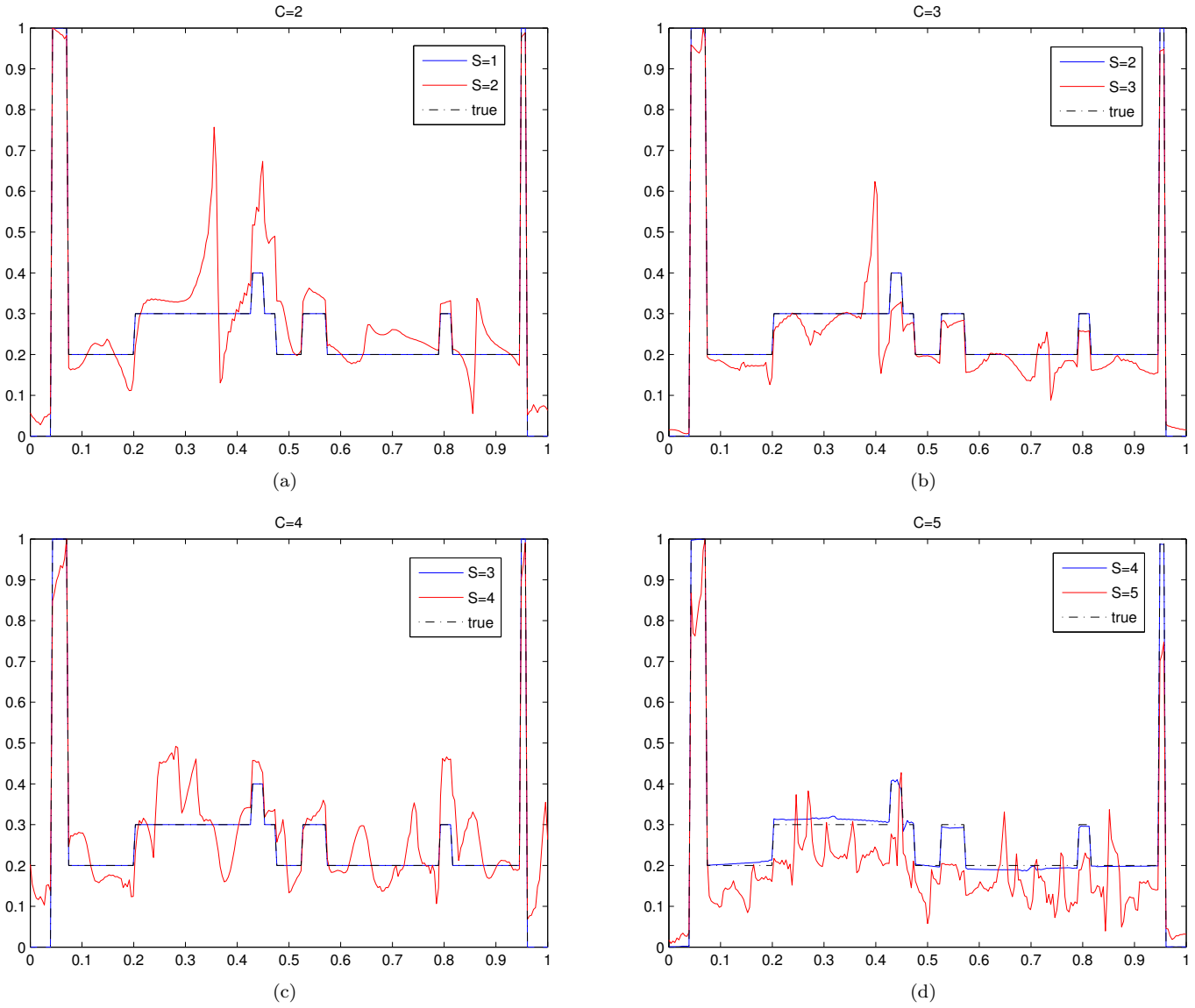

Fig. 4. Reconstructions of one line of a phantom using the proposed method with different coil numbers and acceleration factors: (a) 2 coils, (b) 3 coils, (c) 4 coils, (d) 5 coils. Shown are the true image and two reconstructions from an acceleration factor which is smaller respectively larger than the limiting factor according to (2).

might be large enough (based on the theoretically possible coupling). It is therefore possible, using this relation and an estimate of the energy distribution of the frequencies of image and receiver, to determine the necessary center lines. On the other hand, the numerical method described above can be used for an efficient empirical determination of the required number of center lines.

2) Receivers: An important problem, which we have not understood in a quantitative way yet, is the interdependence between the stability of the proposed method and the receiver configuration. The investigations of this issue up to this point have all been of qualitative nature and yielded the expected results, i.e., that the less linearly dependent the receivers are, the better the method works.

However, the condition number of the matrix described in (3) seems to have a non-trivial dependence on the condition number of the matrix generated by the receivers, $\mathcal{R}$. Part of the cause might be that the solution of the whole problem is not unique up to (at least) a constant, and therefore ill-conditioning is always present, which dominates the (additional) ill-conditioning introduced by a bad choice of the receiver configuration.

It is important to remark that we have to face two opposing effects:

- The smoother the receiver sensitivities relative to the image, the higher the possible acceleration factor. This follows from equation (2)*ff.*
- The rougher the receiver sensitivities in absolute terms, the more receivers one can use (i.e. we have the possibility of higher acceleration factors), and the higher the SNR can be expected to be. This is due to the fact that a set of rougher sensitivities will more likely be linearly independent, and that the coupling between the coefficients of the image and

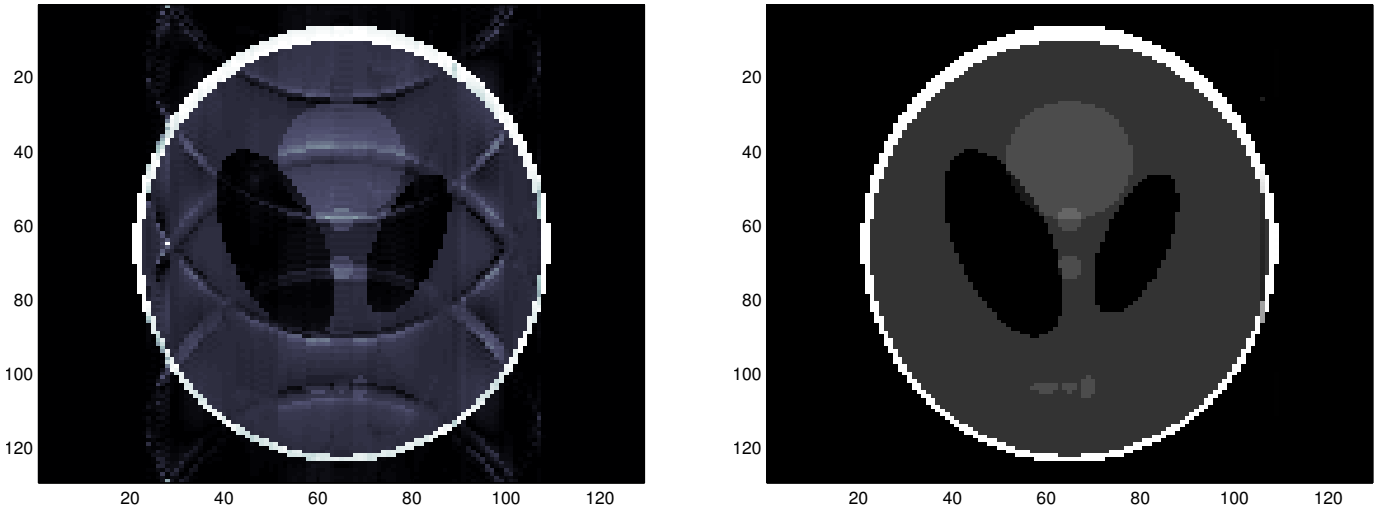

Fig. 5. Reconstruction of a 2D phantom with $N_P = 128, N_R = 6, C = 12, S = 4$: (a) no center lines, (b) 3 center lines.

the measurement (via the non-zero coefficients of the sensitivities) will be stronger (cf. IV-1).

A critical task in parallel imaging is therefore to balance these effects, for which our results can serve as a useful guide.

V. Conclusion

As seen in section III-C, this one-dimensional model together with the numerical method can replicate the features and problems inherent in the reconstruction problem of parallel imaging quite well. For this reason, it can serve as an effective tool in evaluating the feasibility of specific measurement configurations, as specified by the desired resolution, acceleration factor, the smoothness and number of coils, and especially the number of center lines, before committing to a full realization. A failure of the one-dimensional model, which constitutes a "best case" situation, will imply that other algorithms which do not specifically use extra assumptions will give poor and unreliable results as well.

Future work will be concerned with a quantitative estimation of the effect of center lines on the reconstructability of realistic data, and refining the numerical method for use on in vivo data. Furthermore, we expect that different sampling strategies such as radial sampling or subsampled 3D volume acquisition can be treated with a similar approach as well.

Acknowledgment

The authors wish to thank Rudolf Stollberger and Florian Knoll for helpful comments and discussions.

References

[1] Z.-P. Liang and E. M. Haacke, "Biomedical NMR," in *Wiley Encyclopedia of Electrical and Electronics Engineering*, 1999.

[2] D. Weishaupt, V. D. Koechli, and B. Marincek, *How does MRI work? An Introduction to the Physics and Function of Magnetic Resonance Imaging*, 2nd ed. Berlin: Spinger, 2006.

[3] K. P. Pruessmann, M. Weiger, M. B. Scheidegger, and P. Boesiger, "SENSE: Sensitivity encoding for fast MRI," *Magnetic Resonance in Medicine*, vol. 42, pp. 952–962, 1999.

[4] M. A. Griswold, P. M. Jakob, and R. M. Heidemann, "Generalized autocalibrating partially parallel acquisitions (GRAPPA)," *Magnetic Resonance in Medicine*, vol. 47, pp. 1202–1210, 2002.

[5] L. Ying and J. Sheng, "Joint image reconstruction and sensitivity estimation in SENSE (JSENSE)," *Magnetic Resonance in Medicine*, vol. 57, no. 6, pp. 1196–1202, 2007.

[6] F. Bauer and S. Kannengiesser, "An alternative approach to the image reconstruction for parallel data acquisition in MRI," *Math. Methods Appl. Sci.*, vol. 30, no. 12, pp. 1437–1451, 2007.

[7] M. Uecker, T. Hohage, K. T. Block, and J. Frahm, "Image reconstruction by regularized nonlinear inversion - joint estimation of coil sensitivities and image content," *Magnetic Resonance in Medicine*, vol. 60, no. 3, pp. 674–682, 2008.

[8] F. Wiesinger, P. Boesiger, and K. P. Pruessmann, "Electrodynamics and ultimate SNR in parallel MR imaging." *Magn Reson Med*, vol. 52, no. 2, pp. 376–390, 2004 Aug.

[9] F. Wiesinger, P.-F. Van de Moortele, G. Adriany, N. De Zanche, K. Ugurbil, and K. P. Pruessmann, "Potential and feasibility of parallel MRI at high field," *NMR in Biomedicine*, vol. 19, no. 3, pp. 368–378, 2006.

[10] D. K. Sodickson and C. A. McKenzie, "A generalized approach to parallel magnetic resonance imaging," *Medical Physics*, vol. 28, pp. 1629–1643, 2001.

[11] M. A. Ohliger and S. D. K., "An introduction to coil array design for parallel MRI," *NMR in Biomedicine*, vol. 19, no. 3, pp. 300–315, 2006.

[12] J. B. Son and J. X. Ji, "Auto-calibrated dynamic parallel MRI with phase-sensitive data." *Conf Proc IEEE Eng Med Biol Soc*, vol. 1, pp. 751–754, 2006.

[13] C. B. García and T. Y. Li, "On the number of solutions to polynomial systems of equations," *SIAM J. Numer. Anal.*, vol. 17, no. 4, pp. 540–546, 1980.

[14] A. B. Bakushinskij, "The problem of the convergence of the iteratively regularized Gauss-Newton method," *Comput. Math. Math. Phys.*, vol. 32, pp. 1353–1359, 1992.

[15] E. J. Candès, J. Romberg, and T. Tao, "Robust uncertainty principles: exact signal reconstruction from highly incomplete frequency information," *IEEE Trans. Inform. Theory*, vol. 52, no. 2, pp. 489–509, 2006.